AIAA JOURNAL
Vol. 39, No. 8, August 2001

Reduced-Order Models for Nonlinear Unsteady Aerodynamics

Daniella E. Raveh*
Georgia Institute of Technology, Atlanta Georgia 30332-0150

Reduced-order models (ROM), which are based on the Volterra theory for nonlinear systems, for the evaluation of nonlinear unsteady aerodynamic forces are presented. The ROMs provide a means for rapid evaluation of frequency-domain generalized aerodynamic forces, which can then be used in traditional flutter analysis schemes to calculate flutter characteristics about nonlinear steady flows. Two ROMs are formulated, an impulse-type ROM that is based on the convolution of ROM kernels with the input signal, and a step-type ROM that is based on convolution with the derivative of the input signal. Linear, first-, and second-order kernels are identified for these two ROMs from direct computational fluid dynamics (CFD) impulse and step responses. The ROM methodology is demonstrated with the heave and elastic modes of the AGARD 445.6 wing. It was found that the accuracy of the CFD-based impulse response is dependent on the choice of input amplitude and computational time step and that the impulse-type kernels are highly sensitive to inaccuracies in the impulse responses used for their identification. The step-type ROM was found to be robust and resulted in good predictions of the direct responses. The introduction of second-order kernels did not significantly improve the predictions, indicating a difficulty in performing true nonlinear identification. The use of first-order, step-type ROM offered a significant computational time saving compared to the full CFD frequency response analysis.

Introduction

RECENT studies introduced the concept of reduced-order models (ROMs) for nonlinear aerodynamics. This concept suggests that the input–output relation of a complex computational fluid dynamics (CFD) system (that is, flow equations and boundary conditions) can be represented by a relatively simple mathematical model, which is the ROM. Feeding an arbitrary input signal through the ROM is far more efficient than feeding it through the full CFD analysis, and yet the response captures the physical characteristics of the nonlinear system.

Different approaches for reduced-order modeling of aerodynamic systems include linearization about a nonlinear steady-state condition (e.g., Refs. 1 and 2), linear model fitting [such as the Autoregressive Moving Average (ARMA) model in Ref. 3], representation of the aerodynamic system in terms of its eigenmodes (e.g., Ref. 4), and representation of the aerodynamic system using the Volterra theory of nonlinear systems (e.g., Ref. 5). The latter ROM method is the focus of the current study.

The Volterra theory of nonlinear systems[6] states that the response of a nonlinear system to an arbitrary input can be evaluated by multidimensional convolution integrals, each of which is associated with an internal kernel function. A central issue in the application of the Volterra theory is the identification of these kernel functions. This is typically done based on some known system's input–output relations. Once the kernels are identified, the response to an arbitrary input can be evaluated in a straightforward manner using convolution schemes.

The use of the Volterra theory for modeling aerodynamic systems was first suggested by Silva,[5,7–10] who implemented a direct kernel identification method based on the system response to impulse inputs. The method was demonstrated for a plunging and pitching rigid wing using the CAP-TSD transonic small disturbance code[9] and for a plunging airfoil using the CFL3D Navier–Stokes (NS) code.[5]

With the aim of identification of the aerodynamic system based on test data, Reisenthel and Bettencourt[11] and Reisenthel[12] introduced an indirect kernel identification method. This approach suggests expanding the unknown kernels on some known basis function set, for example, decaying exponentials, and solving for the basis function coefficients based on input–output relations. In this approach, the difficulties associated with the realization of the inputs are eliminated. However, the method requires many sets of input–output relations (to be used directly or for training purposes), to assure the correct identification of the system kernels. Kurdila et al.[13] and Prazenica et al.[14] also addressed the problem of approximation of Volterra kernels based on general input–output relations by using wavelet approximation.

A recent study by Raveh et al.[15] presented a linearized ROM for the evaluation of unsteady aerodynamic forces in response to arbitrary modal motion. In this study, the system's step responses served as the ROM's kernels. The ROM was used to compute generalized aerodynamic force (GAF) matrices, at different values of reduced frequencies, which were then used in flutter analysis. The method was demonstrated on the AGARD 445.6 wing,[16] comparing flutter characteristics to those reported from wind-tunnel tests and from flutter analyses based on linear aerodynamic theories. The study provided some guidelines to the creation of the linearized ROM and also identified some of the prediction limitations of the linearized ROM.

The purpose of Ref. 15 was to provide a proof of concept for the use of Volterra-theory ROMs for GAF matrices evaluation and flutter analysis. Therefore, important issues such as 1) the details of kernel identification, 2) the differences between impulse-based and step-based ROMs, and 3) first- vs second- vs higher-order models were not addressed in great detail. The current study expands on the scope of Ref. 15 by addressing in detail these issues, which are critical for successful modeling.

The application of the Volterra theory to aerodynamic systems, and especially the approach of direct kernel identification, are relatively new and not thoroughly studied. The current paper is a summary of experiments of different approaches for ROM generation. It presents the successful modeling attempts as well as the unsuccessful ones, with the purpose of expanding the knowledge on the applicability of reduced-order modeling of nonlinear unsteady aerodynamic systems.

Volterra Theory ROM

The Volterra theory (see Ref. 6) formulates the input–output relation of a nonlinear time-invariant system. For a discrete system, the response $y[n]$ to an arbitrary input signal $u[n]$ can be evaluated by a multidimensional convolution as

Received 5 July 2000; revision received 1 February 2001; accepted for publication 8 March 2001.

*Research Engineer, School of Aerospace Engineering. Member AIAA.

$$y[n] = h_0 + \sum_{k=0}^{n} h_1[n-k]u[k] + \sum_{k1=0}^{n}\sum_{k2=0}^{n} h_2[n-k1, n - k2]u[k1]u[k2] + \cdots + \sum_{k1=0}^{n}\cdots\sum_{kn=0}^{n} h_n[n-k1, \ldots, n - kn]u[k1]\cdots u[kn], \qquad n = 0, 1, 2, \ldots \tag{1}$$

where n is the discrete-time variable, h_0 is the steady-state response, and the functions $h_n[n-k1, \ldots, n-kn]$ are the Volterra kernels of the system.

For small perturbations about the steady-state condition, the system response can be considered linear. In such a case, the system's response is given by

$$y[n] = \sum_{k=0}^{n} h_1[n-k]u[k], \qquad n = 0, 1, 2, \ldots \tag{2}$$

where the steady-state response h_0 was assumed to be zero. Equation (2) represents a first-order Volterra system in which $h_1[n-k]$ is the first-order kernel. For a linear (or linearized) system $h_1[n-k]$ is also the system's impulse response, that is, the response to a unit impulse, which in a discrete-time system is defined as

$$\delta[n] = \begin{cases} 1.0 & \text{for} \quad n = 0, \\ 0.0 & \text{for} \quad n \neq 0, \end{cases} \qquad n = 0, 1, 2, \ldots \tag{3}$$

The first-order kernel of a first-order Volterra system can be directly identified simply by feeding the impulse input of Eq. (3) to the system and recording the response. In realistic numerical applications, the impulse input may be of a physical amplitude ξ_0, in which case the first-order kernel is the normalized impulse response:

$$h_1[n] = (1/\xi_0)y_0[n], \qquad n = 0, 1, 2, \ldots \tag{4}$$

where $y_0[n]$ is the system's impulse response.

Equation (2), with the kernel h_1 of Eq. (4), can be used to approximate the response of the nonlinear system, that is, beyond the range of small amplitudes. For the nonlinear system, the first-order kernel $h_1[n-k]$ computed from the impulse response $y_0[n]$ is not unique but rather dependent on the amplitude ξ_0. Consequently, the predicted response to an arbitrary input will be sensitive to the choice of ξ_0.

For a higher level approximation, the nonlinear system can be considered as a second-order Volterra system, for which the response is given by

$$y[n] = \sum_{k=0}^{n} h_1[n-k]u[k] + \sum_{k1=0}^{n}\sum_{k2=0}^{n} h_2[n-k1, n - k2]u[k1]u[k2], \qquad n = 0, 1, 2, \ldots \tag{5}$$

The second-order kernel $h_2[n-k1, n-k2]$ has multiple components, and each component corresponds to a certain $k1$ and $k2$ values (for elaborate discussion of the second-order kernel see Ref. 10). Each component can be identified from the system's response to a double impulse occurring at times $k1$ and $k2$ as follows. The unit-impulse response of the second-order Volterra system is [from Eq. (5)]

$$y0[n] = h_1[n] + h_2[n, n] \tag{6}$$

and the double-impulse response is

$$\begin{aligned} y1[n] &= h_1[n-k1] + h_2[n-k1, n-k1] + h_1[n-k2] \\ &\quad + h_2[n-k2, n-k2] + 2h_2[n-k1, n-k2] \\ &= y0[n-k1] + y0[n-k2] + 2h_2[n-k1, n-k2] \end{aligned} \tag{7}$$

from which the second-order kernel $h_2[n-k1, n-k2]$ can be extracted as

$$h_2[n-k1, n-k2] = \tfrac{1}{2}(y1[n] - y0[n-k1] - y0[n-k2]) \tag{8}$$

Only two measurements (responses), $y0$ and $y1$, are required to compute one component of the second-order kernel. This is because the system is time invariant, and therefore, $y0[n-k1]$ is the same as $y0[n-k2]$ shifted by the time $(k1-k2)$. The identification of each additional component requires another measurement of a double-impulse response.

The second-order kernel represents the second-order memory of the nonlinear system. For example, it can be seen from Eq. (8) that the component $h_2[n-1, n-2]$ equals the difference between the response to a double impulse at time steps 1 and 2 and the sum of the responses to single impulses at times 1 and 2. For a linear system (first-order memory only) this difference would equal zero. For a system with finite second-order memory, only the first few components of the second-order kernel are significant. Therefore, the identification effort is limited to these first few components. It is shown in the numerical example section that, for the Euler system considered, only the first few components (three or four) of the second-order kernel are significant and need to be identified.

The first-order kernel of the system can be defined by interpolation, using an additional response of a different amplitude. From Eq. (5), the response to an impulse of amplitude ξ_0 is

$$y2[n] = \xi_0 h_1[n] + \xi_0^2 h_2[n, n] \tag{9}$$

Combining Eqs. (6) and (9) yields the expression for the first-order kernel:

$$h_1[n] = \frac{\xi_0^2 y0[n] - y2[n]}{\xi_0^2 - \xi_0} \tag{10}$$

Note that this kernel is different than the first-order kernel of the first-order system [Eq. (4)]. The first-order kernel of a second-order system is a weighted average of responses to different amplitudes and can be thought of as an equivalent first-order kernel. It can be used with the linear approximation [Eq. (2)] to provide the best nonlinear representation over an amplitude range of interest.

Step-Type ROM

An alternative approach presented in this paper is to compute the response of the nonlinear system from multiple convolutions of step-type kernels with the derivative of the input signal. A first-order approximation, using the step-type ROM, is formally written as

$$y[n] = \sum_{k=0}^{n} s_1[n-k](u[k] - u[k-1]), \qquad n = 0, 1, 2, \ldots \tag{11}$$

and the second-order approximation is

$$y[n] = \sum_{k=0}^{n} s_1[n-k](u[k] - u[k-1]) + \sum_{k1=0}^{n}\sum_{k2=0}^{n} s_2[n-k1, n-k2](u[k1] - u[k1-1])(u[k2] - u[k2-1]), \qquad n = 0, 1, 2, \ldots \tag{12}$$

in which $s_1[n-k]$ and $s_2[n-k1, n-k2]$ are the first- and second-order, step-type kernels. They can be identified following the same procedure that was described in the preceding section, replacing the impulse responses by step responses.

A question that needs to be answered is why is the introduction of a step-type ROM necessary, when we have already established the impulse-type ROM? One reason is that the CFD analysis of a step response is less prone to numerical problems and that the identification of step-type kernels is less sensitive to such errors. This will be demonstrated in the results section. The other reason is that in a nonlinear system, a single-impulse response does not fully characterize the system.[17] Thus, the use of steps in a first-order ROM

or in a second-order ROM with a limited number of retained kernel components results in more accurate predictions. This can be seen by considering the single step and impulse responses of a second-order system. The impulse response of a second-order system is given by Eq. (6), and the step response [from Eq. (5)] is

$$y_{\text{step}}[n] = \sum_{k=0}^{n} h_1[n-k] + \sum_{k1=0}^{n}\sum_{k2=0}^{n} h_2[n-k1, n-k2]$$

$$n = 0, 1, 2, \ldots \quad (13)$$

It can be seen that the impulse response of Eq. (6) does not fully characterize the second-order system because it is only dependent on the diagonal terms of h_2. The step response, on the other hand, does contain all of the first- and second-order kernel components. Note that in a purely second-order system, all of whose kernels are identified, step-type and impulse-type ROMs should be interchangeable, as they are in linear systems.

Results and Discussion

The ROM methodology of this study is studied with the AGARD 445.6 wing. The AGARD 445.6 wing was tested for flutter characteristics in the Transonic Dynamic Tunnel at NASA Langley Research Center[16] and was used as a test case in many studies of nonlinear unsteady aerodynamics.[3,18,19]

The flow is analyzed by the EZNSS[20] NS/Euler code. EZNSS provides the choice between two implicit algorithms, the Beam and Warming algorithm[21] or the partially flux-vector splitting algorithm of Steger et al.[22] Finite differences in the framework of structural computational meshing are used in the discretization process. Grid generation and intergrid connectivity are handled using the chimera approach. Details about the computational grid and steady-state flow results for the AGARD 445.6 wing are presented in Ref. 15.

Validation Test Case

The purpose of the validation test is to validate the numerical procedures of the CFD response to harmonic, impulse and step inputs, the kernel identification process, and the convolution schemes. Another objective is to pinpoint numerical issues associated with the CFD analysis of impulse/step responses. The validation test case is performed using the wing's heave mode at a Mach number of 0.3. The aerodynamic response to the heaving motion is associated only with the heaving velocities and not with both the displacements and velocities, as it is in the other modes. Thus, using the heave mode allows one to study separately the effects of various parameters, such as displacement amplitudes and computational time step, on the response. A low subsonic Mach number was chosen to avoid any physical nonlinear effects that may interfere with possible numerical effects.

Figure 1 presents normalized impulse and step responses to an input with amplitudes of $1e{-}4$ and $1e{-}3$, respectively, that were computed using a nondimensional time step of 0.01. The heave mode was normalized such that a modal displacement of 1 corresponds to a physical displacement of 1 in. (2.54 cm). The impulse and step responses were collected over 1000 CFD iterations, that is, time steps; however, because the decay is very rapid, only the first six time steps are presented in Fig. 1. The sea-level far-field pressure of $p_\infty = 2116.22$ lb/ft^2 (101,327 Pa) was used in the CFD analysis to compute the dimensional forces of Fig. 1 and throughout this study. The responses of Fig. 1 are used as the linear kernels in the convolution schemes of Eq. (2) (impulse) and Eq. (11) (step) to evaluate the response to a sinusoidal excitation with a modal amplitude of $1e{-}1$ and a frequency of 40 Hz (arbitrarily chosen). Comparison of the convolved and direct harmonic responses, presented in Fig. 2, shows that the first-order kernels (both step and impulse) very accurately predicted the direct response. Whereas this example validates the kernel identification process and convolution schemes, the impulse and step parameters that were used (that is, the amplitude and time step) were carefully chosen. It is next demonstrated that the impulse-type ROM is highly sensitive to the selection of these parameters, which may lead to very poor predictions compared to that of Fig. 2.

Effect of Computational Time Step

CFD time-accurate applications typically have a maximum time step that is set based on stability limits or on a reference timescale. The stability limit is commonly determined by the Courant–Friedrichs–Lewy (CFL) number (see Ref. 23). For explicit schemes, a CFL number that is less than unity is used, whereas for implicit CFD schemes, as the one of this study, the CFL number can be much higher than one, that is, larger time steps can be used. The

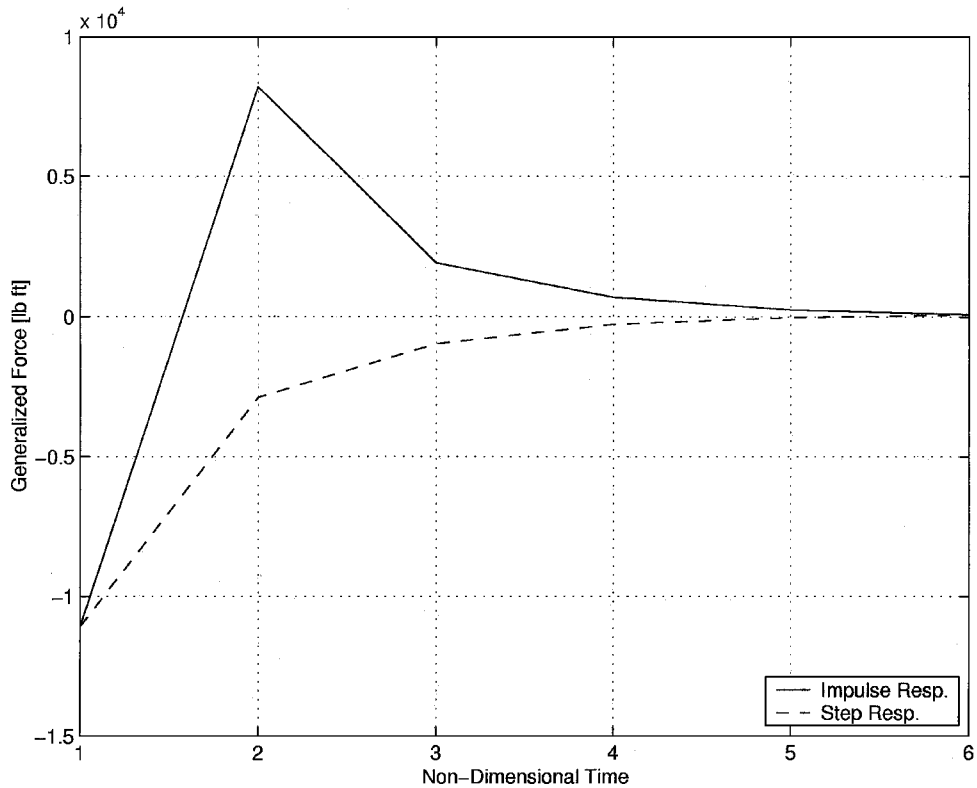

Fig. 1 Impulse and step responses of the heave mode, Mach 0.3; based on input amplitudes of $1e-4$ and $1e-3$, respectively, and time step of 0.01.

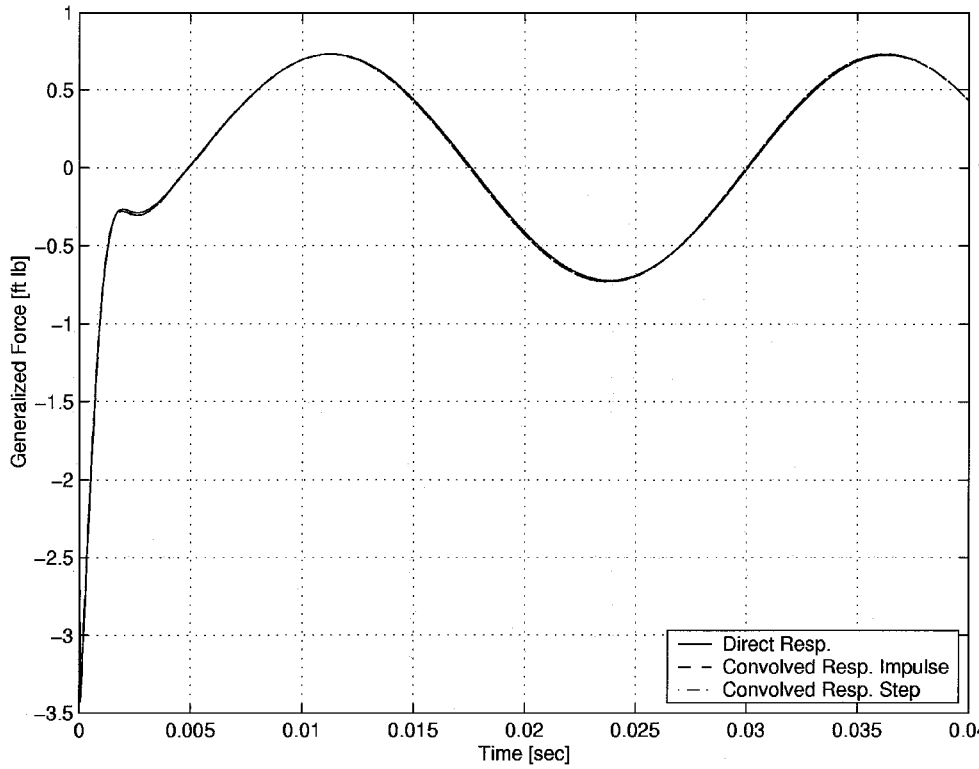

Fig. 2 Convolved vs direct response to sinusoidal excitation of the heave mode, 40 Hz, modal amplitude of $1e-1$, and Mach 0.3.

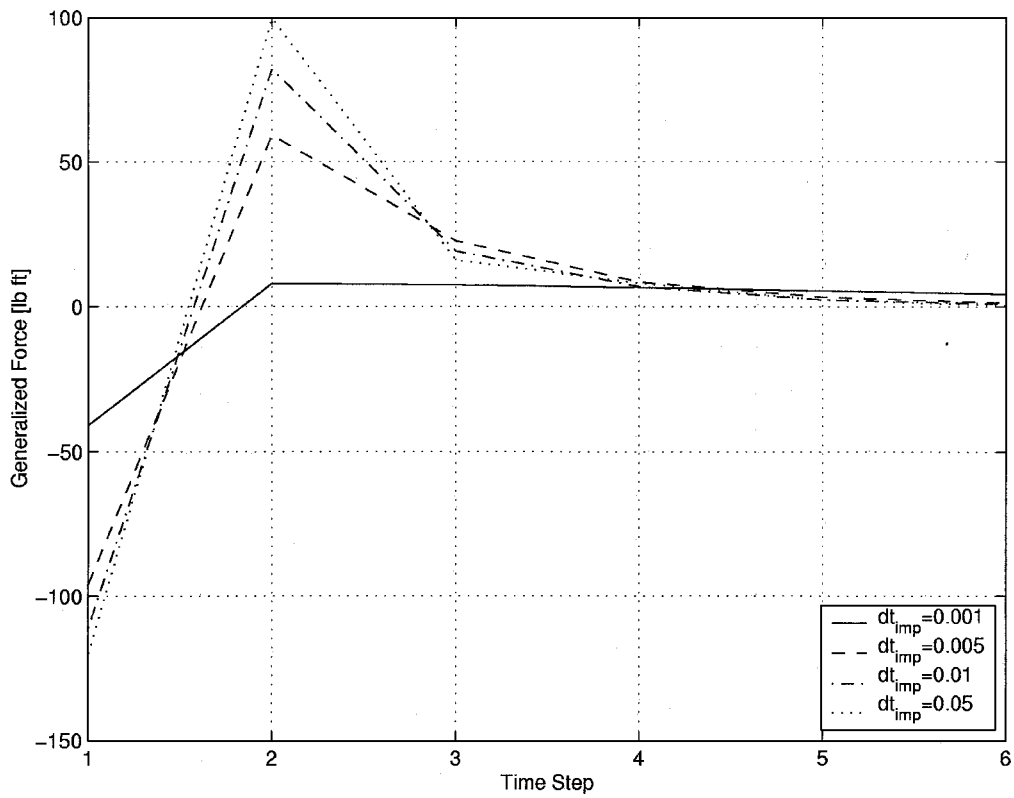

Fig. 3 Impulse responses of the heave mode, Mach 0.3; based on input amplitude of $1e-3$ and varying time steps.

reference timescale is usually 2–3 orders of magnitude smaller than a problem-dependent characteristic time. For example, the response to forced harmonic excitation at a frequency of $f = 40$ Hz is calculated using a time step of 0.0279, which leads to 1000 steps per cycle [based on the dimensionless cycle time of 27.9, computed by $A_{\text{inf}}/f \times L_{\text{ref}}$ using the reference sea-level speed of sound $A_{\text{inf}} = 1116.44$ ft/s (340.3 m/s) and a reference length of $L_{\text{ref}} = 1$ ft (30.48 cm)]. For step/impulse responses there are no established limits on the usable time step, except for the stability limit. The sensitivity of step/impulse responses to variations in time step is investigated next by experimenting with different time steps, keeping the input amplitude fixed.

Figure 3 presents responses to an impulse with an amplitude of $1e-3$ that were computed using time steps of 0.05, 0.01, 0.005, and 0.001. The plots were normalized by multiplying them by the time step. In this manner all of the responses correspond to the

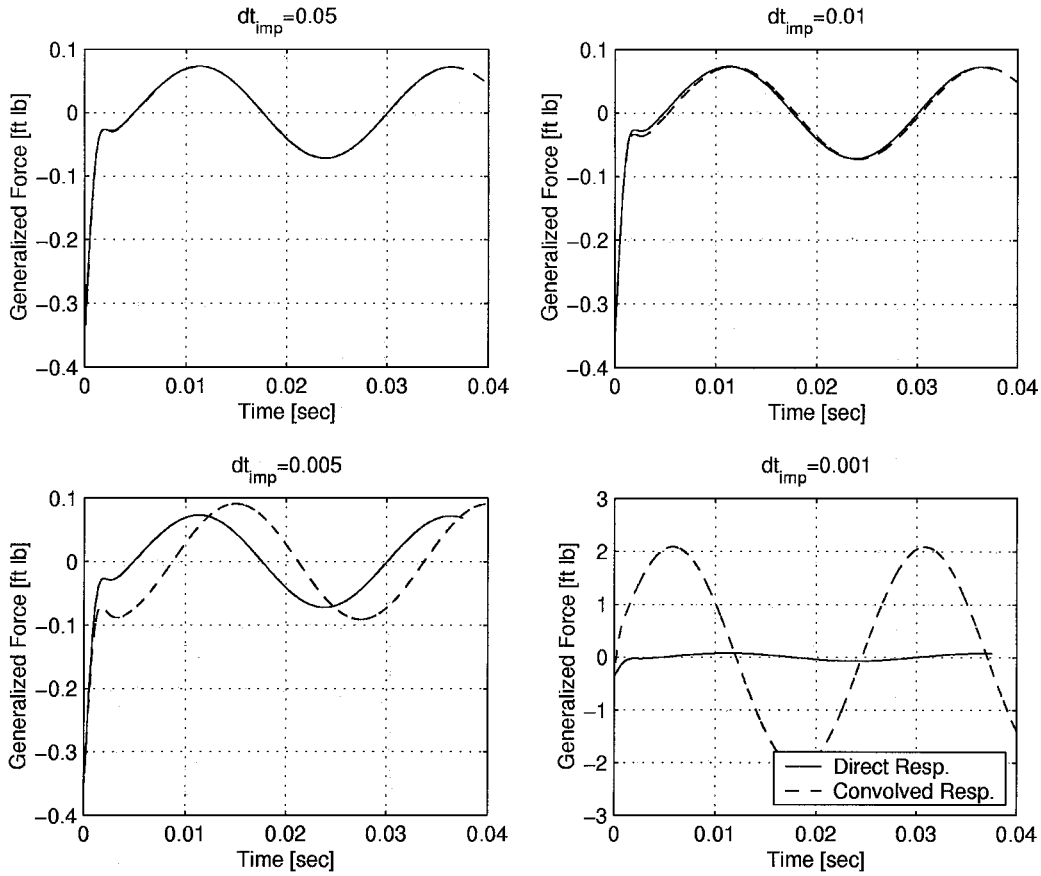

Fig. 4 Convolved vs direct response to sinusoidal excitation of the heave mode, 40 Hz, modal amplitude 1*e*− 2, Mach 0.3; based on impulse responses of fixed amplitude of 1*e*− 3 and varying time steps.

same heaving input velocity. The different impulse responses were used as kernels to predict the forced harmonic response shown in Fig 4. The impulse that resulted in the best prediction is the one based on the largest time step. When the time step was decreased, the convolved response deteriorated. Although increasing the time step seemed to improve the response, the time step could not be increased beyond the value of 0.05 because this resulted in numerical instabilities. This behavior seems counterintuitive because typically in CFD applications, smaller time steps are associated with increased accuracy rather than a loss of accuracy.

This behavior can possibly be explained by considering the numerical nature of the CFD scheme. The computational scheme has a certain propagation speed that is set by the spatial and time discretizations. When an impulse input is introduced to the CFD computation, the grid is displaced by a certain displacement over a time period equal to the computational time step. This results in a grid velocity that equals the displacement divided by the time step, and thus a smaller time step results in higher velocity. When this velocity exceeds the integration speed of the numerical scheme, then the numerical scheme is incapable of accurately propagating the disturbance, and the accuracy of the response deteriorates.

Also note that the larger the time step the shorter the computational time of the convolution. Although the computational time of all of the convolved responses of Fig. 4 is negligible compared to that of the direct CFD response, the convolved response based on the 0.001 time step took about 50 times longer than the one based on the 0.05 time step.

Effect of Input Amplitude

Next is considered the effect of the input amplitudes on the impulse responses. Because the test is performed in the linear aerodynamics regime, the normalized responses are expected to be independent of the input amplitudes. Figure 5 presents impulse responses (first six time steps of each response) that were computed using a dimensionless time step of 0.01 and modal amplitudes of 1*e*−4, 1*e*−3, 5*e*−3, and 1*e*−2. Figure 5 presents the normalized responses, that is, the responses divided by their input amplitudes.

In the large scale, the different responses seem to be congruent. Zoom-in reveals discrepancies between the responses, where the larger the amplitude, the smaller the response. This behavior supports the hypothesis that was presented before, that the larger the interference velocity, that is, the larger the amplitude, when based on the same time step, the less accurate the CFD response. This seemingly small difference has a dramatic effect on the convolved response. Figure 6 presents the convolved vs direct responses to sinusoidal excitation at modal amplitudes of 1*e*−2, 1*e*−1, and 1 (columns 1–3 in Fig. 6, respectively). The convolved responses are based on the impulse responses of Fig. 5. The title of each plot in Fig. 6 indicates the impulse modal amplitude ξ_{imp} and the harmonic input amplitude ξ. The convolved responses that are based on the impulses of small amplitudes resulted in very good agreement with the direct responses, regardless of the amplitude of the direct excitations (first and second rows). As the impulse amplitudes are increased, discrepancies between the convolved and direct responses grow larger (third and fourth rows) indicating that the impulses that correspond to the larger amplitudes are inaccurate. The impulse-based predictions (convolved responses) appear to be extremely sensitive to the accuracy of the impulse responses, thus making the impulses less favorable for use in Volterra ROMs.

Second-order kernels were computed from Eq. (8) based on impulses of different amplitudes. When the small-amplitude impulses were used, in which case the normalized responses were identical, the identified second-order kernels were practically zero, as they should be in the linear regime. Using the larger amplitude impulses, which are associated with numerical errors, nonzero second-order kernels resulted. These second-order kernels, which are not physical in the linear aerodynamics regime, resulted in erroneous convolved responses, even if the kernels themselves were of a very small magnitude.

Finally, the effect of the impulse velocity increment was examined by comparing the cases shown in Fig. 7, which have the same

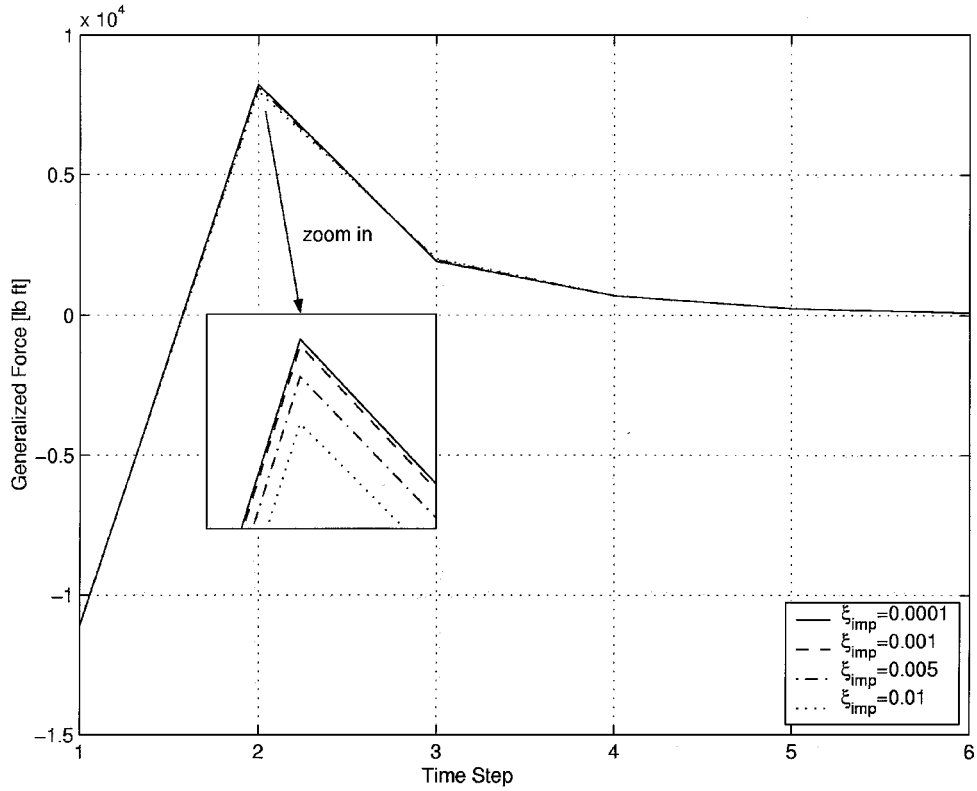

Fig. 5 Impulse responses of the heave mode, Mach 0.3; based on time step of 0.01 and varying input amplitudes.

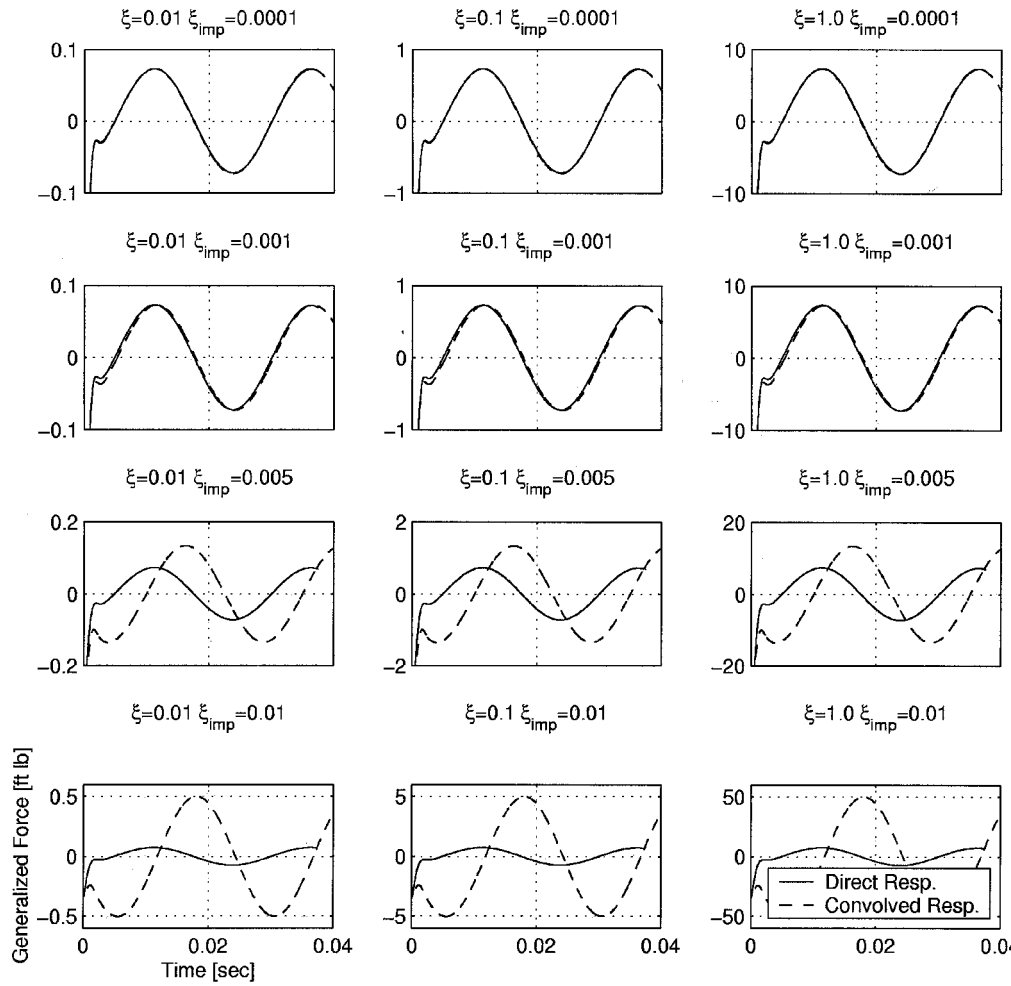

Fig. 6 Convolved vs direct response to sinusoidal excitation of the heave mode, 40 Hz, Mach 0.3; based on impulse responses of fixed time step of 0.01 and varying amplitudes.

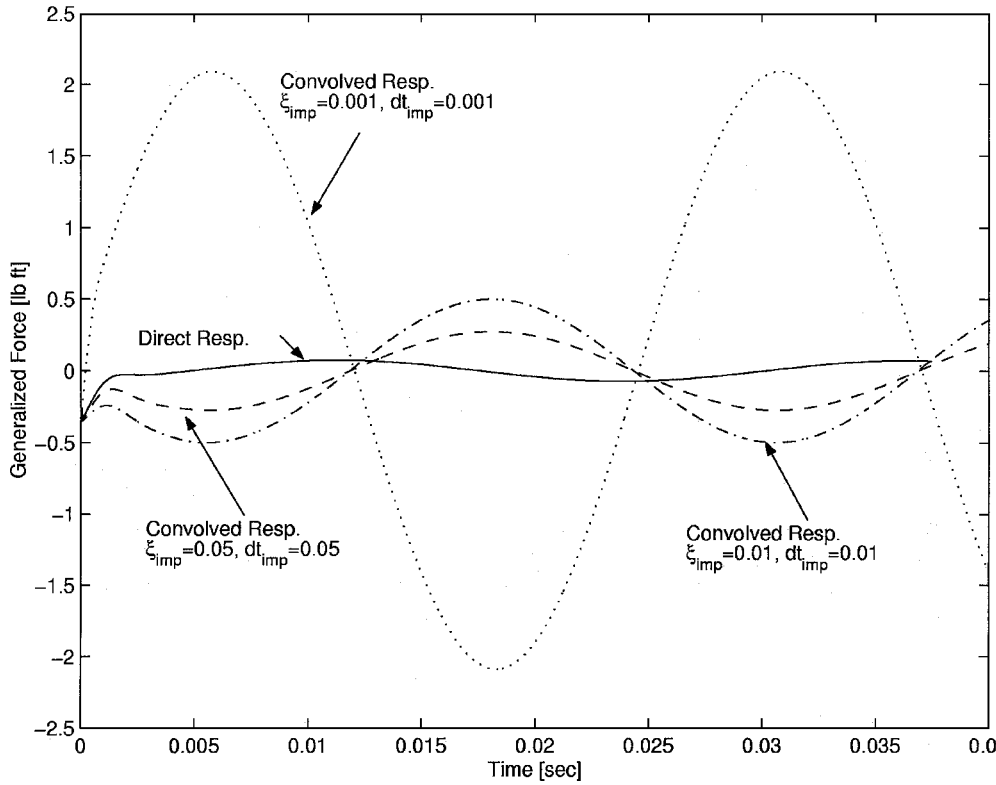

Fig. 7 Convolved vs direct response to sinusoidal excitation of the heave mode, 40 Hz, modal amplitude $1e-2$, Mach 0.3; based on impulses of the same velocity and different time steps.

velocities but different time steps. The velocity used to predict the response of Fig. 7 was too high to produce good prediction, no matter what the time step. It is seen, however, that as the time step was decreased, the quality of the prediction deteriorated. This behavior supports the hypothesis that there is a numerical limit to the increments of interference, both displacements and velocities, for which the numerical scheme is capable of accurately propagating the interference. It is possible that an analytical criterion for the minimum time step can be formulated in a similar manner to the formulation of the stability criterion (CFL number condition) for the maximum time step. This is, however, beyond the scope of this paper.

Linear Step-Type Kernels

Figure 8 presents the convolved vs the direct responses to sinusoidal excitation at a frequency of 40 Hz and modal amplitudes of $1e-2$, $1e-1$, and 1 (columns 1–3 in Fig. 8, respectively). These are the same responses of Fig. 6 except that the convolved responses were computed from Eq. (11) using step responses. The dimensionless time step dt_{st} and modal amplitude ξ_{st} used to compute the different step responses are indicated in the title of each plot. Also indicated is ξ, the forced-harmonic input amplitude. In the first row the step has the same parameters as the impulse that was used to compute the responses shown in the last row of Fig. 6. Unlike in the impulse case, the convolved responses agree very well with the direct responses. This is because the step signal is inherently associated with smaller velocity and velocity increments (in the first time step the impulse and step have the same velocity, but in the second time step the step input has no velocity). In the second row it is seen that, when the velocity is increased, discrepancies between the convolved and direct responses start to show up. In the last row the time step is decreased, that is, the velocity is the same as in the second row but the velocity increment is increased, the step response worsens, and the predicted response becomes erroneous.

In summary of the observations from the validation test cases, it was found that there are numerical limitations that restrict the impulse/step maximum input amplitude and minimum time step that can be accurately handled by the CFD numerical scheme. These limits are very restrictive for impulse response analyses and less restrictive for step responses. The impulse-type ROMs were also found to be very sensitive to inaccuracies in the identified kernels, thus making them less favorable for Volterra ROM applications. It should be emphasized that the specific limits indicated here are relevant to the particular CFD code and application of this study.

Second-Order ROMs

Next, second-order ROMs are computed from impulse and step responses and used to predict linear and nonlinear aerodynamic responses. To avoid confusion, it is restated that the second-order ROM is associated with first- and second-order kernels and that the first-order kernel of the second-order ROM is different from the first-order kernel of a first-order (linear) ROM. The ROMs in this subsection are all second order. CFD responses to harmonic excitation of the heave mode at Mach 0.9, a frequency of 40 Hz, and modal amplitudes of $\xi = 1$ and 5 serve as the reference for the convolved responses. The $\xi = 5$ response is not exactly five times the 1.0 response, indicating some nonlinearity at this level of excitation. It, therefore, serves as the reference nonlinear response.

Various impulse responses were computed, corresponding to amplitudes ranging from $1e-5$ to $1e-1$ and computational time steps of 0.01 and 0.05. Pairs of these impulses were used in Eq. (10) to identify first-order kernels. Convolved responses based on these kernels are shown in Fig. 9, with the legend indicating the impulse amplitudes used for identification. The first-order kernels of the nonlinear system are dependent on the impulse amplitudes, unlike the linear system's kernels, which are amplitude independent. This results in the differences between the convolved responses that can be observed in Fig. 9. A correlation exists between the quality of the predicted response and the input velocities of the impulse signals. It is possible that a first-order kernel based on impulses of larger amplitudes would result in a better match between the $\xi = 5$ convolved and direct responses. This, however, was impossible to compute, due to numerical limitations on large impulse amplitudes (as was the case in the validation test). For the same reason it was impossible to identify second-order kernels based on these impulse responses. Whereas the impulses of very small amplitude had no nonlinear content, those based on large amplitudes were infected with numerical inaccuracies. Examination of Eq. (8), which is used for the identification of second-order kernels, reveals that the latter are based

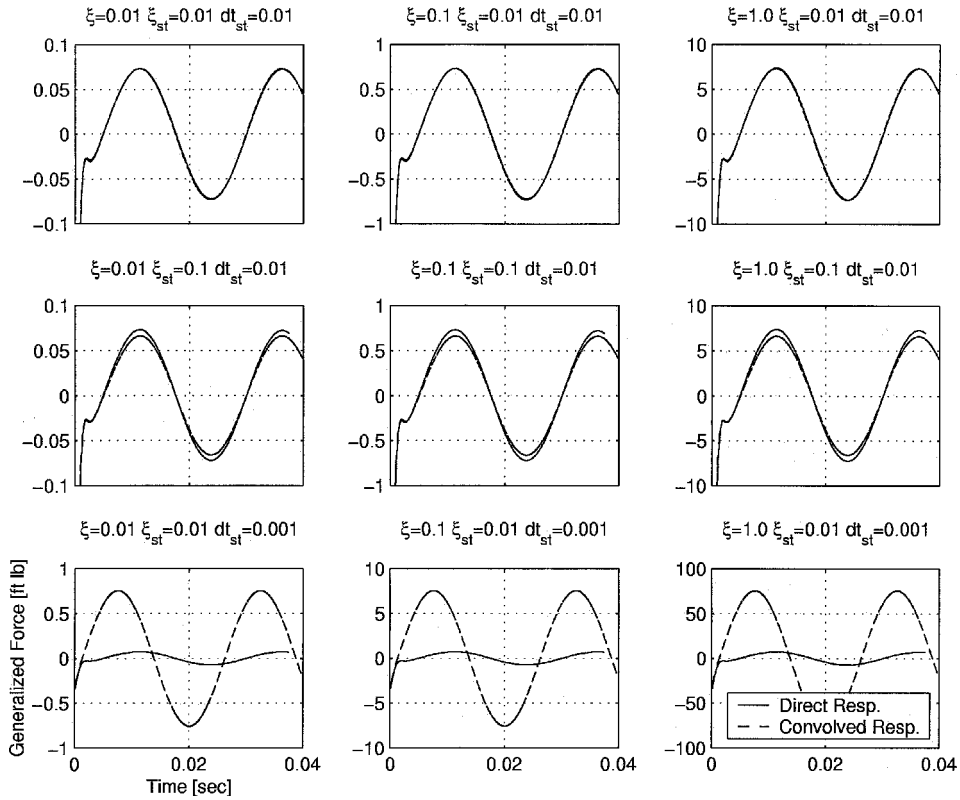

Fig. 8 Convolved vs direct response to sinusoidal excitation of the heave mode, 40 Hz, Mach 0.3; based on step responses of different time steps and input amplitudes.

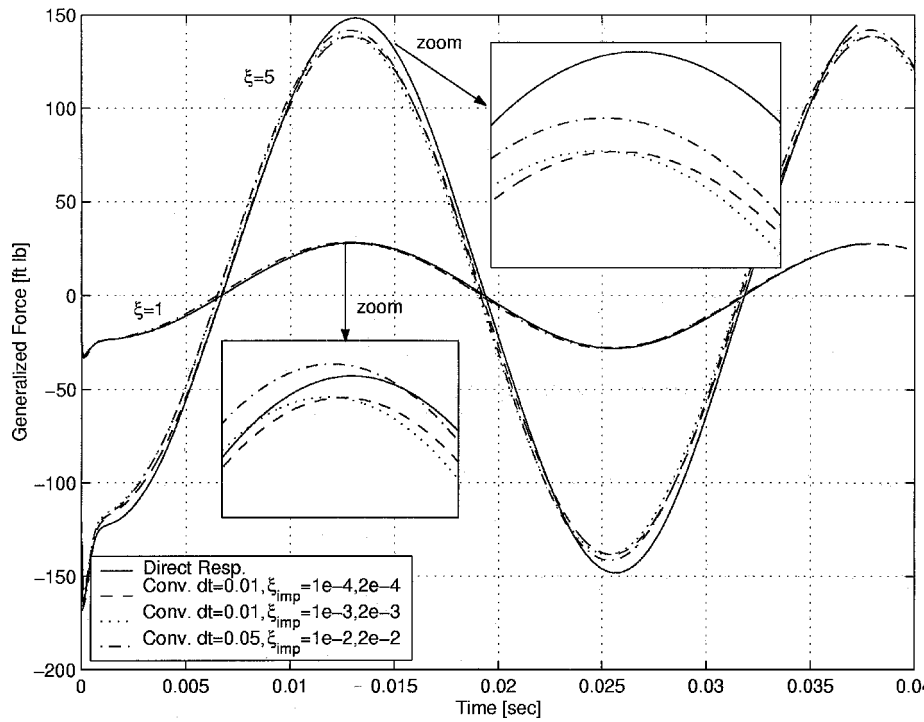

Fig. 9 Convolved vs direct response to sinusoidal excitation of the heave mode, 40 Hz, Mach 0.9; based on first-order kernels of second-order ROMs from impulse responses.

on the differences between normalized impulse responses. These differences are typically small and in this application were found to be on the order of magnitude of the numerical errors. Moreover, the nature of convolution, that is, the summation of elements, makes the convolved response highly sensitive to inaccuracies in the kernels. This characteristic was pointed out for the first-order kernel, in the validation test, and applies also for the second-order kernels.

First- and second-order kernels were identified from step responses and used to compute the convolved responses shown in Fig. 10. The CFD application of step responses permits more freedom in increasing the step amplitude without encountering numerical problems. From these responses, second-order kernels can be identified. Only the first four components of the second-order kernel, shown in Fig. 11, were identified and accounted for. The identification of these kernels was based on five responses to the following signals: a step of amplitude $1e-2$ at time step 1; a step of amplitude $2e-2$ at time step 1; and a double impulse of amplitude $1e-2$ at time steps 1 and 2, 1 and 3, and 1 and 4. All step responses were

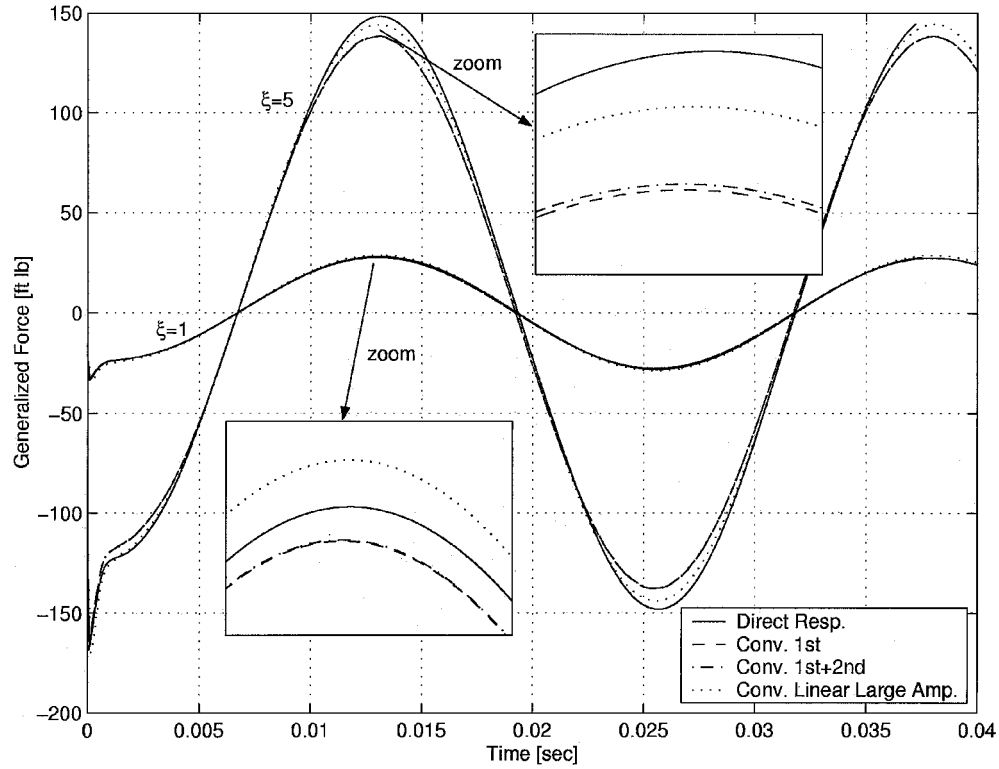

Fig. 10 Convolved vs direct responses to sinusoidal excitation of the heave mode, 40 Hz, Mach 0.9; based on first- and second-order kernels from step responses.

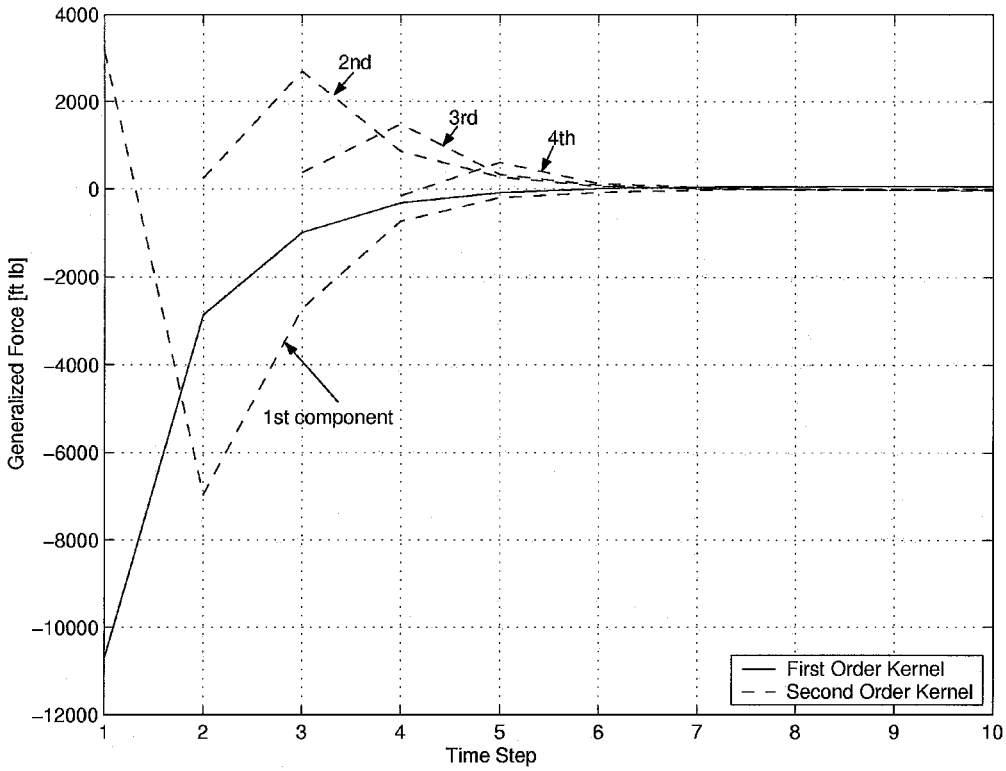

Fig. 11 First-order kernel and four components of the second-order kernel of the heave mode, Mach 0.9.

computed using a time step of 0.01. The size of the second-order kernel components is significantly smaller compared to the first-order kernel, and it is decreased from one component to the next, indicating that it is sufficient to identify only the first few components. The convolved responses of Fig. 10 agree very well with the direct response, better than the impulse-based responses that contain a small phase shift. A small gap between the convolved and direct responses exists and was not significantly improved with the introduction of the second-order terms. An even better match between the $\xi = 5$ convolved and direct responses was achieved when a linear kernel, that is, first-order ROM, was used that is based on a step of larger amplitude (0.2, computed with time step of 0.05). This is indicated by the dotted line in Fig. 10. Using this kernel for the $\xi = 1$ case deteriorated the response.

The test case of this section reflects a mildly nonlinear response for which the first-order kernel influences the convolved response

significantly more than the second-order kernels. Being a weighted average of responses, the first-order kernel captures the level of nonlinearity that is associated with the amplitudes that were used for identification (or velocity amplitudes in the case of the heaving motion). Good convolved responses are obtained for signals whose amplitudes are within the range of amplitudes of the identification steps. When a ROM is sought for the evaluation of responses to signals of known amplitudes, a first-order ROM, based on a single step response about that amplitude, can predict the response better than the weighted first-order kernel of a second-order ROM.

ROMs for the Elastic Modes

The four elastic modes, which were calculated by finite element analysis in Ref. 16, were mapped into the CFD surface grid points, using the interface method of Refs. 24 and 25. Figure 12 shows the wing's elastic modes, already mapped to the CFD surface grids, indicating the associated frequencies. The modes are normalized to yield an identity generalized mass matrix.

Because it was already established in the preceding sections that the step-type ROM is more robust and results in better predictions, the following section presents results from step-type ROMs only. Impulse-type ROMs for the elastic modes were created as well, and the results are available from the author. They are not presented due to space limitations.

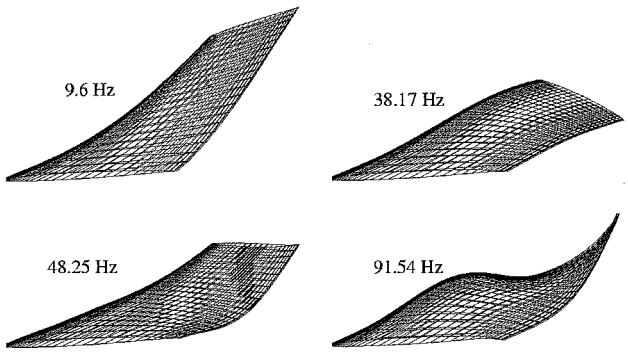

Fig. 12 AGARD 445.6 wing, first four elastic mode shapes mapped into the CFD surface grids.

Figure 13 shows the first wing-bending mode step response at Mach number 0.96. The four plots present the time histories (transients) of the GAFs in the four elastic modes, recorded from the CFD analysis in response to a step of amplitude $1e-3$ introduced to the first mode. This input amplitude corresponds to a maximum tip deflection of about 0.1% of the root chord. The responses of Fig. 13 are normalized by the step amplitude.

Figure 14 presents the convolved vs the direct response (in all four modes) to a sinusoidal excitation of the first mode, at a frequency of 40 Hz and a modal amplitude of $1e-1$. The dashed lines present responses from a first-order ROM. These were computed from Eq. (11), in which the s_1 kernels are the normalized step responses of Fig. 13. The first-order ROM resulted in good prediction of the forced-harmonic response for modes 1, 2, and 4, which are close to linear. The direct response of mode 3, which is nonlinear (this can be seen by the fact that the output signal is not a sinusoid), was not accurately predicted by the first-order ROM. When the system was assumed to be a second-order system, the first-order kernel and first four components of the second-order kernel were identified from Eqs. (10) and (8) using the step and double-step responses to input amplitude of $1e-3$. The convolved second-order response is shown by the dashed dotted line in Fig. 14, where it can be seen that the second-order representation slightly improved the prediction.

First- and second-order ROMs were created also for the first wing-torsion mode input, and evaluated against the direct CFD response to harmonic excitation of that mode at a frequency of 10 Hz and at a Mach number of 1.141. A modal amplitude of $5e-3$ of the input sinusoid was used, which corresponds to a wing-tip rotation angle of about 1.5 deg.

Figure 15 presents convolved vs direct responses, showing three convolved responses that are based on first-order ROMs using step responses of amplitudes $1e-4$, $1e-3$, and $5e-3$. All three first-order ROMs were able to predict the responses of modes 1, 3, and 4 very well. The different predictions of the second mode response are attributed to the different step amplitudes. It is evident that the best prediction is obtained when the step amplitude is the closest to the direct forced-harmonic input amplitude.

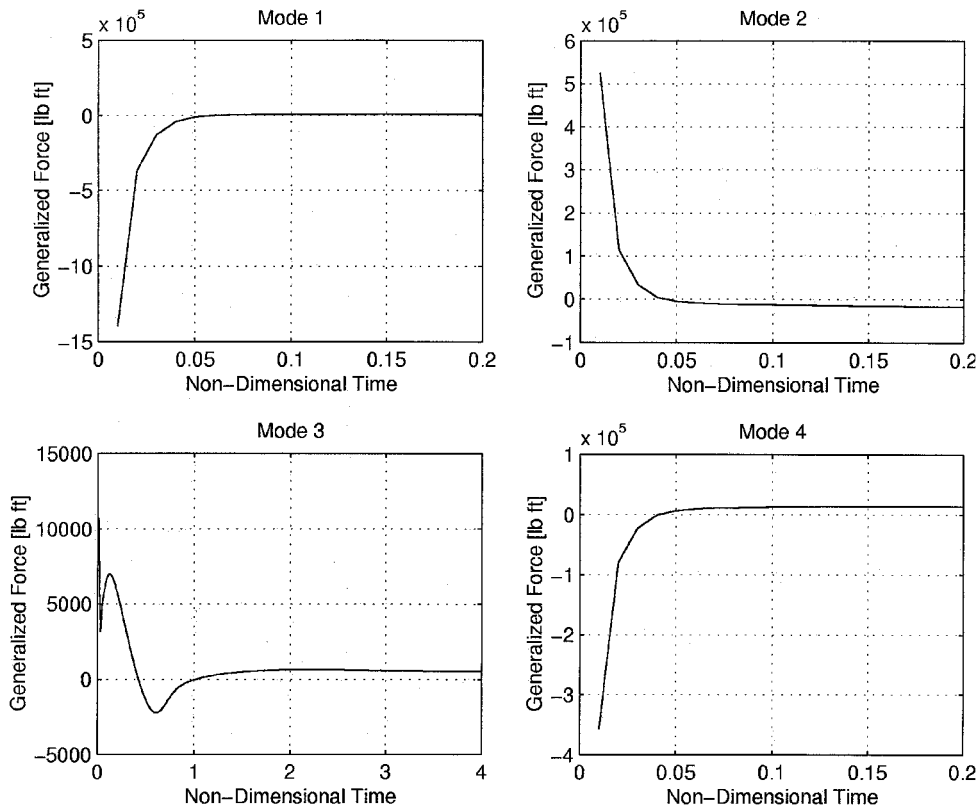

Fig. 13 Recorded CFD response to $1e-3$ step in the first wing-bending mode, Mach 0.96.

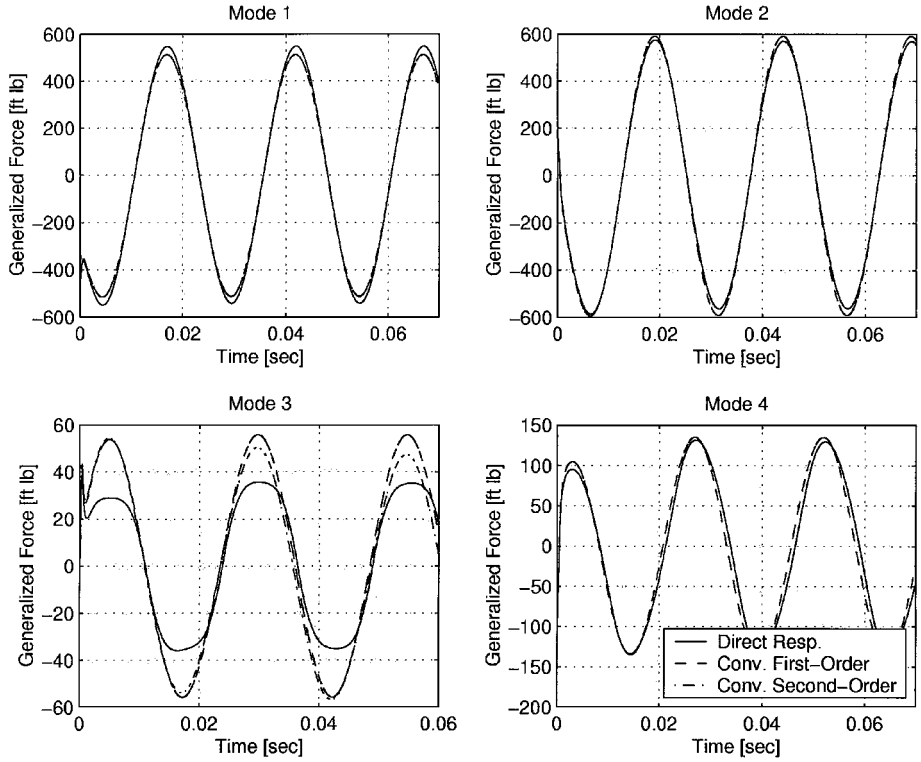

Fig. 14 Convolved vs direct response to sinusoidal excitation of the first wing-bending mode, 40 Hz, modal amplitude 1*e*− 1, Mach 0.96; based on first- and second-order, step-type ROM.

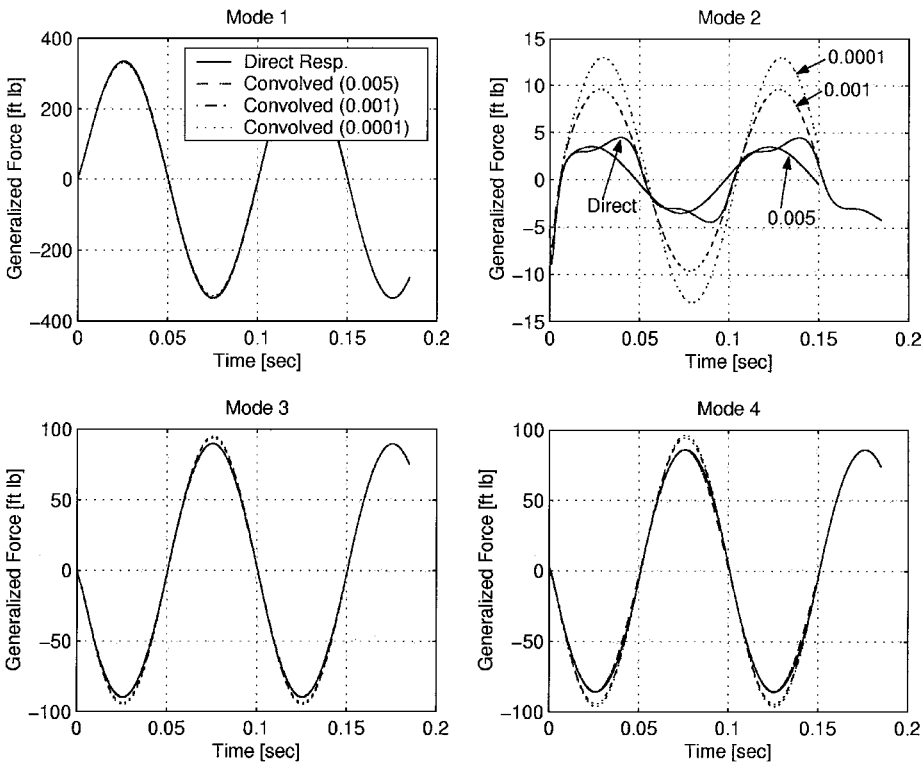

Fig. 15 Convolved vs direct response to sinusoidal excitation of the first wing-torsion mode, 10 Hz, modal amplitude 5*e*− 3, Mach 1.141; based on first-order, step-type ROMs.

When the system is assumed to be a second-order system, the first-order kernel and first four components of the second-order kernel shown in Fig. 16 were identified from the step and double-step responses to input amplitude of 1*e*−3. Figure 17 presents the convolved vs the direct response based on these kernels. When Fig. 17 is compared to Fig. 15, it is seen that assuming the system to be of second-order did not improve the prediction and that the contribution of the second-order kernel components was negligible compared to that of the first-order kernel.

The evaluation of first- and second-order ROMs in this section is limited to two modes at two frequencies and at two Mach numbers. A sweep on frequencies from zero to about 150 Hz, for various Mach numbers, was presented in Ref. 15, based on first-order ROMs only. Results of Ref. 15 show that for the most part the first-order step-type ROMs produce GAFs in agreement with linear aerodynamic theory and wind-tunnel tests. The introduction of second-order ROMs in this study was aimed at improving the predictions in those nonlinear cases. The failure of second-order ROMs to improve significantly

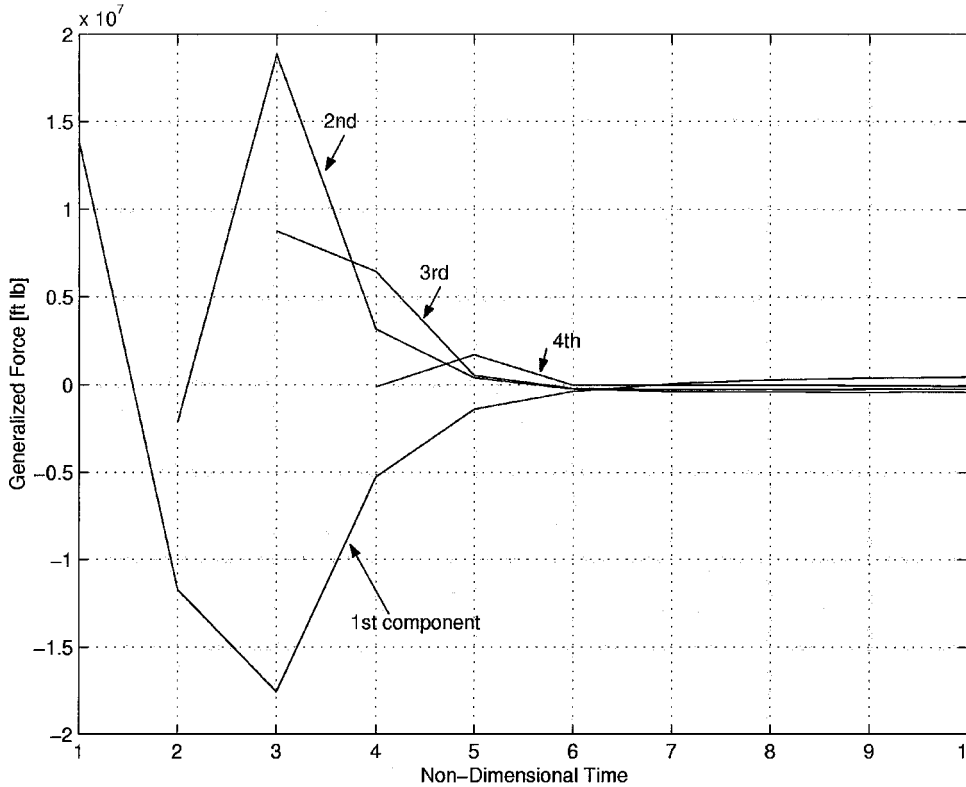

Fig. 16 Four components of the second-order kernel of the first wing-torsion mode, Mach 1.141.

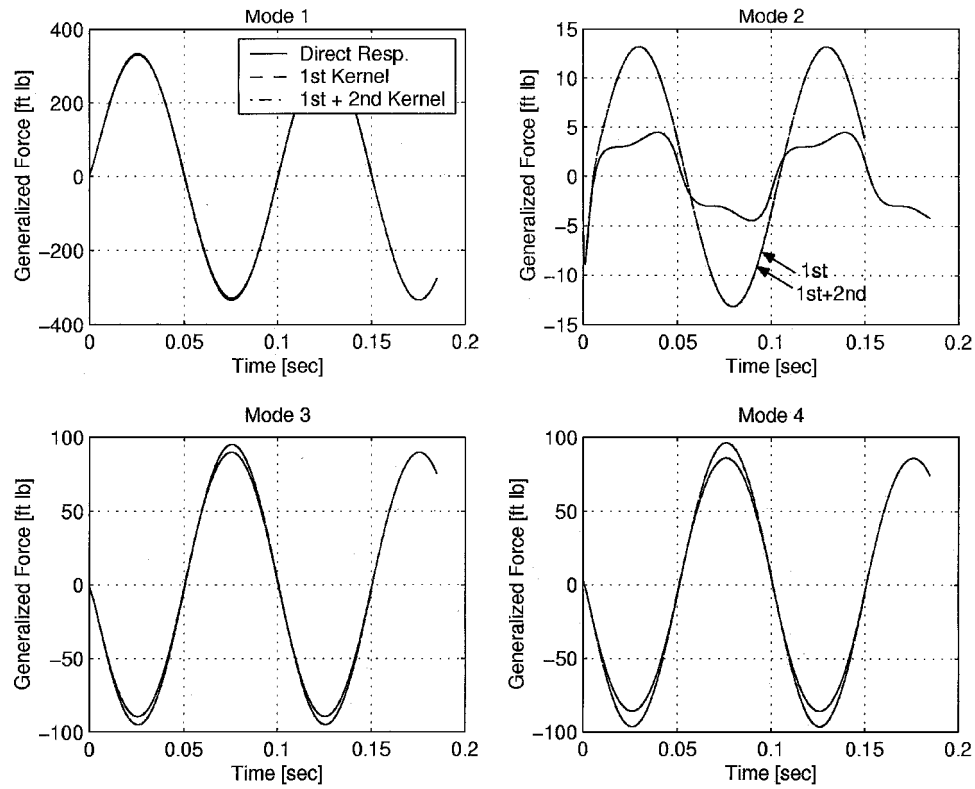

Fig. 17 Convolved vs direct response to sinusoidal excitation of the first wing-torsion mode, 10 Hz, modal amplitude 5*e*− 3, Mach 1.141; based on a second-order, step-type ROM.

the predictions may be unique to this application, but it may also point to a general difficulty to perform true nonlinear identification.

Finally, note that the use of ROMs, especially when limited to first-order, offers significant computational time saving compared to the full CFD frequency response analysis. For the test case of this study, the computation of step/impulse responses, at a specific Mach number and for one mode, required 1000 CFD iterations. Based on these responses, the frequency response can be evaluated within a few minutes. For comparison, the direct CFD response over one cycle at one frequency of 10 Hz required approximately 4000 CFD iterations.

Summary

The paper presented two reduced-order-modeling approaches for the evaluation of nonlinear GAFs based on CFD computations. First- and second-order, impulse-type and step-type ROMs were identified

and used to evaluate the generalized unsteady aerodynamic forces in response to forced-harmonic modal motions (heave plus four elastic modes) of the AGARD 445.6 wing.

It was found that, when the nonlinear system is represented as a first- or second-order Volterra system, it is difficult to identify correctly the system's kernels from impulse responses. CFD impulse responses were found to be highly sensitive to the choice of input amplitude and time step, resulting in inaccurate responses to sharp impulses, that is, too large amplitudes over too small time steps. Convolved response, based on impulse-type ROMs, were found to be extremely sensitive to inaccuracies in the impulses that are used for identification.

The CFD step response was proven to be less sensitive to the choice of input amplitude and time step, and the step-type ROMs resulted in very good predictions of the forced-harmonic responses in the linear regime or for small excitations. In cases at which the direct response was nonlinear, the first-order step ROM did not predict very accurately the amplitude of the response. However, it was found that the prediction accuracy was improved as the step amplitude was closer to that of the direct excitation signal. Assuming the system to be second-order did not significantly improve the ROM. The first-order kernels of the second-order ROM, which are different than the kernels of the first-order system, dominate the responses, and the addition of second-order kernels did not significantly improve the prediction, if at all. The failure of second-order ROMs to improve the predictions significantly may be unique to this application, but it may also point to a general difficulty to perform true nonlinear identification.

The first-order, step-type ROM, which was found in this study to accurately predict mildly nonlinear responses, can be used to evaluate rapidly the frequency-domain GAF coefficients. These can then be integrated into a traditional frequency-domain flutter analysis, to predict flutter characteristics about a nonlinear steady flow, as was demonstrated in Ref. 15. The first-order kernel of a second-order system, which is a weighted average of step responses of different amplitudes, can be used as an equivalent first-order ROM to capture at best the nonlinear response over an amplitude range of interest.

Finally, note that the ROMs of this study, although they are valid only to one configuration and Mach number, offer significant time savings compared to the full CFD forced-harmonic response, especially when used to compute responses over a range of frequencies.

Acknowledgments

The author extends thanks to W. Silva of NASA Langley Research Center and M. Karpel of Technion—Israel Institute of Technology, for their assistance in discussion of the results presented in this paper.

References

[1]Ballhaus, W. F., and Goorjian, P. M., "Computation of Unsteady Transonic Flows by Indicial Methods," *AIAA Journal*, Vol. 16, No. 2, 1978, pp. 117–124.

[2]Lee-Rausch, E. M., and Batina, J. T., "Wing Flutter Boundary Prediction Using Unsteady Euler Aerodynamic Method," *Journal of Aircraft*, Vol. 32, No. 2, 1995, pp. 416–422.

[3]Cowan, T. J., and Arena, A. S., Jr., and Gupta, K. K., "Accelerating CFD-Based Aeroelastic Predictions Using System Identification," *Proceedings of the 36th AIAA Atmospheric Flight Mechanics Conference and Exhibit*, AIAA, Reston, VA, 1998, pp. 85–93.

[4]Dowell, E. H., "Eigen-Mode Analysis in Unsteady Aerodynamics: Reduced-Order Models," *Proceedings of the 36th Structures, Structural Dynamics, and Materials Conference*, AIAA, Reston, VA, 1995, pp. 2545–2557.

[5]Silva, W. A., "Reduced-Order Models Based on Linear and Nonlinear Aerodynamic Impulse Response," *International Forum on Aeroelasticity and Structural Dynamics*, NASA Langley Research Center, Hampton, VA, 1999, pp. 369–379.

[6]Rugh, W. J., *Nonlinear System Theory. The Volterra/Wiener Approach*, Johns Hopkins Univ., Baltimore, MD, 1981, pp. 3–21.

[7]Silva, W. A., "Application of Nonlinear Systems Theory to Transonic Unsteady Aerodynamic Responses," *Journal of Aircraft*, Vol. 30, No. 5, 1993, pp. 660–668.

[8]Silva, W. A., "Extension of a Nonlinear System Theory to General-Frequency Unsteady Transonic Aerodynamic Responses," *Proceedings of the 34th Structures, Structural Dynamics, and Materials Conference*, AIAA, Washington, DC, 1993, pp. 2490–2503.

[9]Silva, W. A., "Identification of Linear and Nonlinear Aerodynamic Impulse Response Using Digital Filter Techniques," *Proceedings of the 35th AIAA Atmospheric Flight Mechanics Conference*, AIAA, Reston, VA, 1997, pp. 584–597.

[10]Silva, W. A., "Discrete-Time Linear and Nonlinear Aerodynamic Impulse Responses for Efficient CFD Analyses," Ph.D. Dissertation, Dept. of Applied Mechanics, College of William and Mary, Williamsburg, VA, Oct. 1997.

[11]Reisenthel, P. H., and Bettencourt, M. T., "Extraction of Nonlinear Indicial and Critical State Responses from Experimental Data," *Proceedings of the 37th AIAA Aerospace Sciences Meeting and Exhibit*, AIAA, Reston, VA, 1999.

[12]Reisenthel, P. H., "Prediction of Unsteady Aerodynamic Forces via Nonlinear Kernel Identification," *International Forum on Aeroelasticity and Structural Dynamics*, NASA Langley Research Center, Hampton, VA, 1999.

[13]Kurdila, A., Prazenica, C., Rediniotis, O., and Strganac, T., "Multiresolution Methods for Reduced Order Models for Dynamical Systems," *Proceedings of the 40th Structures, Structural Dynamics, and Materials Conference*, AIAA, Reston, VA, 1999, pp. 649–658.

[14]Prazenica, R., Kurdila, A., and Silva, W., "Multiresolution Methods for Representation of Volterra Series and Dynamical Systems," *Proceedings of the 41st Structures, Structural Dynamics, and Materials Conference* [CD-ROM], AIAA, Reston, VA, 2000.

[15]Raveh, D. E., Levy, Y., and Karpel, M., "Aircraft Aeroelastic Analysis and Design Using CFD-Based Unsteady Loads," *Proceedings of the 41st Structures, Structural Dynamics, and Materials Conference* [CD-ROM], AIAA, Reston, VA, 2000.

[16]Yates, E. C., Jr., "AGARD Standard Aeroelastic Configurations for Dynamic Response. Candidate Configuration I.-Wing 445.6," NASA TM-100492, 1987.

[17]Schetzen, M., *The Volterra and Wiener Theories of Nonlinear Systems*, Wiley, New York, 1980, pp. 44–46.

[18]Cunningham, H. J., Batina, J. T., and Bennett, R. M., "Modern Wing Flutter Analysis by Computational Fluid Dynamics Method," *Journal of Aircraft*, Vol. 25, No. 10, 1988, pp. 962–968.

[19]Lee-Rausch, E. M., and Batina, J. T., "Wing Flutter Computations Using an Aerodynamic Model Based on the Navier–Stokes Equations," *Journal of Aircraft*, Vol. 33, No. 6, 1996, pp. 1139–1147.

[20]Raveh, D. E., Levy, Y., and Karpel, M., "Structural Optimization Using Computational Aerodynamics," *International Forum on Aeroelasticity and Structural Dynamics*, NASA Langley Research Center, Hampton, VA, 1999, pp. 469–481.

[21]Beam, R. M., and Warming, R. F., "An Implicit Factored Scheme for the Compressible Navier–Stokes Equations," *AIAA Journal*, Vol. 16, 1978, pp. 393–402.

[22]Steger, J. L., Ying, S. X., and Schiff, L. B., "A Partially Flux-Split Algorithm for Numerical Simulation of Unsteady Viscous Flows," *Workshop on Computational Fluid Dynamics*, Inst. of Nonlinear Sciences, Univ. of California, Davis, CA, 1986.

[23]Hirsch, C., *Numerical Computation of Internal and External Flows*, Vol. 1, Wiley, New York, 1994, pp. 287–289.

[24]Raveh, D. E., and Karpel, M., "Structural Optimization of Flight Vehicles with Computational-Fluid-Dynamics-Based Maneuver Loads," *Journal of Aircraft*, Vol. 36, No. 6, 1999, pp. 1007–1015.

[25]Raveh, D. E., "Integrated Aero-Structural Design of Maneuvering Flexible Flight Vehicles," Ph.D. Dissertation, Aerospace Engineering, Technion—Israel Inst. of Technology, Haifa, Israel, Feb. 1999.

E. Livne
Associate Editor